Exchange narrowing of electron spin resonance in a two-dimensional system*

Peter M. Richards
Sandia Laboratories, Albuquerque, New Mexico 87115

M. B. Salamon
Department of Physics and Materials Research Laboratory, University of Illinois, Urbana, Illinois 61801
(Received 30 May 1973)

Electron-spin-resonance (ESR) measurements are reported in the two-dimensional Heisenberg magnet K_2MnF_4 and compared with a theory developed here. Results are in excellent agreement with calculated values and, we feel, give strong confirmation of recent theories of spin dynamics. The theory treats the linewidth ΔH and line shape in a two-dimensional Heisenberg system by assuming diffusive motion for the long-time dependence of the time correlation functions. The short-time dependence is taken to be Gaussian, and the resulting short- and long-time parts are joined together in a manner similar to that used by Gulley, Hone, Scalapino, and Silbernagel. An angular dependence roughly of the form $\Delta H \propto (3\cos^2\theta - 1)^2 + (\text{const.})$ (θ is the angle of dc field with respect to the perpendicular to the plane) is observed at high temperature, as predicted by the theory. This angular dependence *cannot* be explained by either the secular or nonsecular parts of the second moment. Rather, it is due explicitly to the dominance of wave-vector $q \to 0$ modes in the long-time decay of correlations in a two-dimensional system. As temperature is lowered toward the antiferromagnetic ordering temperature $T_N = 45\,°\text{K}$, the linewidth initially decreases, passes through a minimum, and then increases rapidly near T_N. The angular dependence is also temperature-dependent such that $\Delta H(\theta = 90°)$ becomes less than $\Delta H(\theta = 55°)$ below about 65 K. These features of the temperature dependence are consistent with the theory. Indeed, we find absolute agreement between theory and experiment to within 20% or better at all angles over a broad range of temperature. The theory contains no adjustable parameters since classical dipolar coupling is taken as the sole source of broadening and we use the same exchange constant J as obtained from susceptibility measurements. The room-temperature line shape, which is Lorentzian at $\theta = 55°$ and non-Lorentzian at $\theta = 90°$, and the frequency dependence of ΔH, measured at 9.8 and 23.4 GHz, are also in agreement with theory. Shift of the resonance field with angle has been measured as well. This effect can be explained quantitatively by the net dipolar field and, contrary to the other phenomena, does not, in the main, reflect two-dimensional spin dynamics.

I. INTRODUCTION

The recent discoveries of quasi- one- and two-dimensional magnetic materials[1,2] have renewed interest in exchange-narrowed magnetic resonance as a result of an alteration of the basic features of linewidth and line shape in less than three dimensions. The equation originally derived by Anderson and Weiss[3] and by Kubo and Tomita,[4]

$$\Delta\omega \approx \omega_p^2/\omega_e, \tag{1}$$

($\Delta\omega$ is the linewidth in frequency units, ω_p is the rms dipolar perturbation frequency or, equivalently, the second moment of the line shape, and ω_e is the exchange frequency with $\omega_e \gg \omega_p$) assumes that the exchange-induced fluctuations are sufficiently rapid to average the dipolar field seen by a spin to zero in a time $\tau_c \approx 1/\omega_e$, which is much less than the relaxation time $1/\Delta\omega$. In particular, validity of (1) requires that the power spectrum of the time correlation function $\langle \omega_p(t)\omega_p(0)\rangle$ be finite at frequency $\omega = 0$.

Originally,[3,4] the form

$$\langle \omega_p(t)\omega_p(0)\rangle = \langle \omega_p^2\rangle\, e^{-\omega_e^2 t^2/2} \tag{2}$$

was adopted as a convenient choice which satisfies the above conditions.

In the past few years, however, it has been realized that for long times the temporal correlations are governed by spin diffusion,[5] and thus

$$\lim_{t\to\infty} \langle \omega_p(t)\omega_p(0)\rangle \propto |t|^{-d/2} \tag{3}$$

for d dimensions. The difference between (3) and (2) is not catastrophic for $d=3$ since $t^{-3/2}$ is a sufficiently rapid decay to produce a finite value at $\omega = 0$ for the power spectrum $P(\omega)$ given by

$$P(\omega) = \int_{-\infty}^{\infty} dt \langle \omega_p(t)\omega_p(0)\rangle\, e^{i\omega t}. \tag{4}$$

However, a large effect results in one dimension, since $d=1$ in Eq. (3) leads to $P(\omega) \propto \omega^{-1/2}$ for $\omega \to 0$, and thus Eq. (1) cannot hold since, as mentioned above, it assumes that $P(\omega=0)$ is finite. The linewidth in this case turns out to be considerably larger than given by (1), and the line shape, which is Lorentzian if $P(\omega=0)$ is finite, is appreciably non-Lorentzian. These effects have been well documented in one-dimensional compounds.[6,7]

For $d=2$, there is also a divergence of $P(\omega)$ as $\omega \to 0$, but it is of the weak form $\ln(1/\omega)$ and thus it is not immediately obvious whether there will be a great difference between $d=2$ and $d=3$ in practice. In this paper we explore the two-dimensional case in detail both theoretically and experimentally. We find that the logarithmic divergence is indeed strong enough to produce features peculiar to resonance in two dimensions. The most notable of these is an angular dependence of $\Delta\omega$ which is related neither to that of the total second moment $\langle \omega_p^2 \rangle$ nor to that of the "truncated"[8] second moment $\langle \omega_{pT}^2 \rangle$ which includes only the secular ($M=0$, where M is the change in Zeeman quantum number) part of the perturbation.

The observed dependence is roughly of the form

$$\Delta\omega = \alpha + \beta(3\cos^2\theta - 1)^2, \qquad (5)$$

where θ is the angle between the applied field $\vec{H}$ and the normal to the plane and α and β are appropriate constants. By contrast, both $\langle \omega_p^2 \rangle$ and $\langle \omega_{pT}^2 \rangle$ have a θ dependence such that they are larger at $\theta = \frac{1}{2}\pi$ than at $\theta = 0$, and neither of them possesses a minimum in the neighborhood of the "magic angle" $\theta_c = \cos^{-1}(1/\sqrt{3})$.

This evidence differs from the situation in either three or one dimensions where, in the former case, the angular dependence is that of $\langle \omega_p^2 \rangle$—as long as $\omega_0 \ll \omega_{ex}$ (ω_0 is the resonance frequency)—and in the latter[6] case, it is that of $\langle \omega_{pT}^2 \rangle$. The explanation lies in the fact that for $d=1$ or 2 the correlation $\langle \omega_p(t)\omega_p(0) \rangle$ is dominated by long-spatial-wavelength fluctuations for the times of interest, whereas the second moment, which is $\langle \omega_p(t)\omega_p(0) \rangle$ at $t=0$, contains contributions from all wavelengths. In one dimension, however, all wavelengths produce the same angular dependence due to the simple geometry and it is thus adequate to consider only $\langle \omega_{pT}^2 \rangle$. For $d=2$, to the contrary, there is a sizeable difference between the angular dependence associated with wave vector $q=0$ and with that associated with the sum over all wave vectors

Experimental data are reported for the two-dimensional Heisenberg antiferromagnet K_2MnF_4 at temperatures above the ordering temperature T_N. Comparison is made with the theory presented here and very good agreement is obtained for the angular dependence, absolute value of the linewidth, and the line shape. The agreement is particularly impressive in light of the fact that no adjustable variables are used, the only "free" parameters in the theory being the strength of the perturbation—which is given by the classical dipolar interaction—and the exchange interaction—which is known from susceptibility measurements.[9]

Our results for K_2MnF_4 are similar to those published by Boesch *et al.*[10] on the two-dimensional compounds $(CH_3NH_3)_2MnCl_4$ and $(C_2H_5NH_3)_2MnCl_4$. They observed the same angular dependences, but did not offer an explanation.

II. THEORY

A. General formalism and qualitative discussion

The absorption $\chi''(\omega)$ at a frequency ω of an exchange-narrowed electron spin resonance (ESR) line is given by[4,11]

$$\frac{\chi''(\omega-\omega_0)}{\omega} \propto \mathfrak{F}\left[\exp\left(-\sum_{M=0}^{2}\int_0^t d\tau(t-\tau) \times g_M(\tau)\cos M\omega_0\tau\right)\right], \qquad (6)$$

in which $g_M(\tau)$ is a time correlation function related to that part of the perturbing Hamiltonian which induces a change M in total Zeeman quantum number and ω_0 is the angular resonance frequency. The functions $g_M(\tau)$ are related to the total dipolar correlation function through

$$\langle \omega_p(\tau)\omega_p(0) \rangle = \sum_{M=0}^{2} g_M(\tau)\cos M\omega_0\tau .$$

The symbol $\mathfrak{F}$ indicates Fourier transform at the frequency ω. The temperature T is assumed to be high enough that $\hbar\omega_0/k_BT \ll 1$. All time dependence associated with the Zeeman Hamiltonian is explicitly contained in $\cos M\omega_0\tau$, so the time variation of $g_M(\tau)$ is governed solely by the exchange interaction. The values of M are restricted to 0, 1, 2 because the perturbation (dipolar + anisotropy + hyperfine) in all cases of interest is at most quadratic in the spin operators.

As noted in Eq. (3), spin diffusion leads to the result

$$\lim_{\tau\to\infty} g_M(\tau) \propto |\tau|^{-d/2}. \qquad (7)$$

A consequence[6,12,13] of Eq. (7) is that the upper limit of the $M=0$ integral in Eq. (6) can be extended to ∞ for three dimensions, but not for one and two dimensions. This is equivalent to the statement in Sec. I that the spectral density $P(\omega)$ diverges for $\omega \to 0$ in less than three dimensions. Hence, the line shape is purely Lorentzian (Fourier transform of an exponential decay) only in three dimensions. The limits of the $M=1$ and $M=2$ integrals can be extended to ∞ for all dimensions because of the rapid modulation provided by $\cos M\omega_0\tau$. Thus anomalies associated with less than three dimensions arise primarily from the secular ($M=0$) part.

Before proceeding with a formal analysis, it is instructive to consider the differences between the calculation for $d=2$ as presented here and for $d=1$ as presented elsewhere.[6,12,13] There are two basic points to consider: First, the importance of the short-time behavior of $g_M(\tau)$ and the contribution of the $M \neq 0$ terms; and second, the angular dependence of the linewidth.

In regard to the first point, for one dimension the linewidth is insensitive to short-time behavior and the $M \neq 0$ terms as long as the $M=0$ part is appreciably nonzero. This is because the $\tau^{-1/2}$ dependence for $d=1$ produces a sufficiently strong divergence of $\int_0^t (t-\tau) g_0(\tau)\, d\tau$ for $\tau \to \infty$ that only the coefficient of the asymptotic form in Eq. (7) matters. Also, the nonsecular terms are not overly important at high frequencies—except of course near the magic angle $\cos^{-1}(1/\sqrt{3})$, where $g_0 = 0$ for the dipolar perturbation [see Eq. (14a)]—because, as mentioned, there is no divergence of the $M \neq 0$ integrals. In two dimensions, the divergence is only logarithmic so that the asymptotic form is not as dominant as it is in one dimension; and the behavior of $g_0(\tau)$ before the asymptotic dependence is reached is thus far more important. An obvious corollary is that since short-time behavior has a sizeable influence, the nonsecular ($M \neq 0$) terms are also more important in two dimensions. Hence, a more detailed treatment is required here than for the calculation of the width $\Delta\omega$ in $(CH_3)_4NMnCl_3$ (TMMC), say, since it does not suffice simply to know the $\tau \to \infty$ behavior of $g_0(\tau)$.

The second point concerns the angular dependence of $\Delta\omega$. This comes from anisotropy of the dipolar interaction which enters into the expression for $g_M(\tau)$ in the general form

$$g_M(\tau) \propto \sum_{qq'} F_q^{(M)} F_{q'}^{(-M)} \mathcal{S}_{qq'}^{(M)}(\tau), \tag{8}$$

in which $F_q^{(M)}$ is a dipolar factor and $\mathcal{S}_{qq'}^{(M)}(\tau)$ is a time correlation function involving four spin operators. Complete expressions for the quantities above are given in Appendix A, but for the discussion at hand it suffices to note that, for example,

$$F_q^{(0)} = \sum_j (3\cos^2\theta_{ij} - 1) r_{ij}^{-3} e^{i\vec{q}\cdot\vec{r}_{ij}},$$

where θ_{ij} is the angle between $\vec{r}_{ij}$ and the applied field $\vec{H}$, in which $\vec{r}_{ij}$ is the displacement between lattice sites i and j.

Angular dependence for a one-dimensional system is quite simple since all vectors $\vec{r}_{ij}$ have the same angle θ_{ij}. Thus, in particular, for the dominant secular part, we have $F_q^{(0)} \propto (3\cos^2 - 1)$ *for all values of* q, where θ is the angle between $\vec{H}$ and the chain axis. We stress the q independence of this result for a reason which will become evident shortly. Since the $M \neq 0$ terms are important only near the magic angle where $3\cos^2\theta - 1 = 0$, the linewidth is proportional to a power of $|3\cos^2\theta - 1|$, as has been established.[6]

We discuss angular dependence in a two-dimensional system with the aid of Fig. 1. Spins are located on a plane quadratic lattice perpendicular to the crystal c axis; the field $\vec{H}$ makes a polar angle θ with respect to the c axis and an azimuthal angle φ in the plane with respect to a principal planar axis a for the tetragonal K_2MnF_4 structure. The vector $\vec{r}_{ij}$ is at an angle φ'_{ij} with respect to

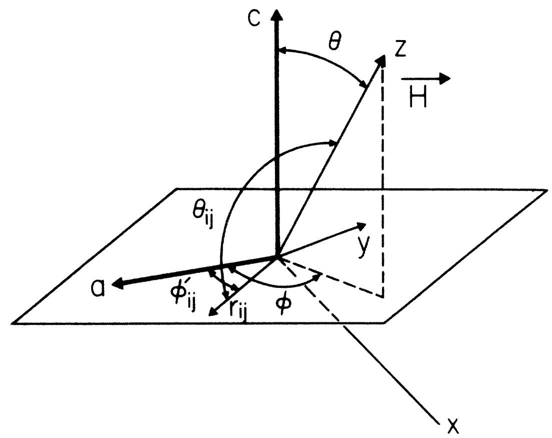

FIG. 1. Coordinate system for planar magnet. The coordinates x, y, z are orthonormal, with y in the plane. The a axis and the displacement r_{ij} also lie in the plane.

the a axis. Thus with respect to the (x, y, z) magnetic field axes, the coordinates of $\vec{r}_{ij}$ are

$$\vec{r}_{ij} = r_{ij}(\cos(\varphi'_{ij} - \varphi)\cos\theta,\ \sin(\varphi'_{ij} - \varphi),\ \cos(\varphi'_{ij} - \varphi)\sin\theta)\,, \tag{9}$$

The quantity $3\cos^2\theta_{ij} - 1$ may be written as

$$3\cos^2\theta_{ij} - 1 = \tfrac{1}{2}(1 - 3\cos^2\theta) + 3[\cos^2(\varphi'_{ij} - \varphi) - \tfrac{1}{2}]\sin^2\theta. \tag{10}$$

Consider now the q dependence of $F_q^{(0)}$. For $q = 0$ we have

$$F_0^{(0)} = \tfrac{1}{2}(1 - 3\cos^2\theta) \sum_j r_{ij}^{-3}\,,$$

which reflects the angular dependence which would be observed if $\mathcal{S}_{qq'}(\tau)$ were dominated by $q, q' \to 0$, which is expected in the $\tau \to \infty$ limit. This result, however, is by no means q independent as may be seen by looking at

$$N^{-1} \sum_q |F_q^{(0)}|^2 = \sum_j r_{ij}^{-6} (3\cos^2\theta_{ij} - 1)^2. \tag{11}$$

With the help of Eq. (10) this becomes

$$N^{-1} \sum_q |F_q^{(0)}|^2 = \tfrac{1}{4}[(1 - 3\cos^2\theta)^2 + 9\sin^4\theta \times (4\langle\cos^4(\varphi'_{ij} - \varphi)\rangle_{av} - 1)] \times \sum_j r_{ij}^{-6}\,. \tag{12}$$

For a continuum, we have $\langle\cos^4(\varphi'_{ij} - \varphi)\rangle_{av} = \frac{3}{8}$; however, for $\varphi = 0$ the value $\langle\cos^4\varphi'_{ij}\rangle_{av} = \frac{1}{2}$ is more nearly correct because this is the case for the four nearest neighbors when H is in the a-c plane, and the r_{ij}^{-6} factor makes nearest neighbors the most important. In either event, we find that the expression (12) is larger at $\theta = \frac{1}{2}\pi$ than at $\theta = 0$. This is not surprising since on the simplest grounds one might expect that the secular contribution would be largest with the field in the plane since then it is possible to realize $\theta_{ij}=0$ at least for some of the spins. [We do find for the special case $\varphi=\frac{1}{4}\pi$, corresponding to $\vec{H}$ in a (110) plane, that $\langle\cos^4(\varphi'_{ij}-\varphi)\rangle\approx\frac{1}{4}$ so that the 3 $\cos^2\theta-1$ dependence is preserved.]

The significance of $\sum_q|F_q^{(0)}|^2$ is that $\mathcal{S}_{qq'}(\tau)\propto\delta_{qq'}$ at $\tau=0$ in the high-temperature limit; so (12) is related to the angular dependence if the short-time behavior of the correlation functions were dominant.

The conclusion is that observation of an angular variation of the form $(3\cos^2\theta-1)^2$ for all azimuthal angles in a two-dimensional system tells us more than it does in a linear chain. Not only does it require that the secular component dominate, but it further shows the interesting fact that the long wavelength $q\to 0$ modes must make up the major contribution. This heavy weighting of $q\to 0$ is consistent with the asymptotic time dependence since the low q modes have the longest lifetimes.

The angular dependences of the $\tau\to 0$ parts $g_0(0)$ and $\sum g_M(0)$ as given by Eqs. (A15)–(A17) are shown in Fig. 2. These represent the secular and complete, secular plus nonsecular, second moments, respectively. It is clear from Fig. 2 that, as mentioned above, the observed angular dependence Eq. (5) cannot be accounted for by the short-time behavior.

B. Calculation of linewidth, infinite temperature

Detailed calculation of the linewidth requires knowledge of the time correlation functions. These are not known exactly so that certain approximations are necessary. The first such approximation is the, by now standard, decoupling of the four-spin correlations into products of two-spin ones.[14–16] In the notation of Eq. (8) this

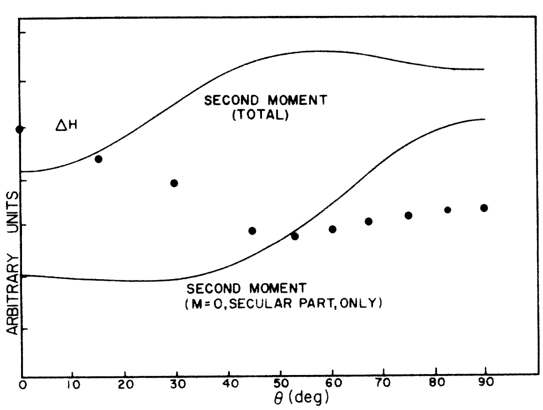

FIG. 2. Theoretical second moments (solid curves) and experimental linewidth (circles) vs angle θ for $\vec{H}$ in a–c plane (100).

amounts to a random-phase approximation (RPA),

$$\mathcal{S}_{qq'}^{(M)}(\tau)=[\phi_q(\tau)]^2\delta_{qq'}\ , \tag{13}$$

where

$$\phi_q(\tau)=3\langle S_q^z(\tau)S_{-q}^z\rangle/S(S+1) \tag{14}$$

and isotropic ($\langle S_q^z(\tau)S_{q'}^z\rangle=\frac{1}{2}\langle S_q^\pm(\tau)S_{q'}^\mp\rangle$) correlations have been assumed. Since there have been, to our knowledge, no detailed improvements to (13) suggested in the literature, it is somewhat difficult to assess the magnitude of the errors which may be involved in the decoupling approximation. It does seem, however, that the remarks in Sec. II A concerning angular dependence are insensitive to the RPA. This is because, for low-dimensional systems, we expect that $\mathcal{S}_{qq'}^{(M)}(\tau)$ is dominated by *both* q and $q'\to 0$ in the $\tau\to\infty$ limit (see Appendix B) so that the $(3\cos^2\theta-1)^2$ dependence of $|F_0^{(0)}|^2$ is preserved irrespective of whether or not (13) is valid. The same argument has been presented regarding angular dependence of linewidth in an antiferromagnet in the critical region.[15]

Next we adopt a procedure somewhat similar to that used by Gulley *et al.*[17] whereby the short-time behavior of $g_M(\tau)$ is approximated by a Gaussian

$$g_M(\tau)=g_M(0)\,e^{-\omega_e^2\tau^2/2}. \tag{15}$$

while the long time behavior is estimated by assuming diffusive decay

$$\phi_q(\tau)=e^{-Dq^2\tau} \tag{16}$$

for the long wavelength modes. We have noted in the above that $\phi_q(0)=3\langle S_q^zS_{-q}^z\rangle/S(S+1)$ is unity, independent of q, in the infinite-temperature limit. Equation (16) is then used in Eqs. (8) and (13) to obtain

$$\lim_{\tau\to\infty}g_M(\tau)=g_M(0)\zeta_M/K\omega_e\tau\ , \tag{17}$$

where

$$\zeta_M\equiv N|F_0^{(M)}|^2\sum_q|F_q^{(M)}|^2,$$

as in (A18) and

$$K\equiv 8\pi D/\omega_e a^2, \tag{18}$$

in which a is the planar lattice constant. Details of the derivation of (17) may be found in Appendix C.

We now seek to describe $g_M(\tau)$ over the whole range by a function which reduces to Eq. (15) for short times and which is given by Eq. (17) for long times. If $\zeta_M\le K/\sqrt{e}$, there exists a finite time τ_M at which the expressions (15) and (17) are equal, whereas if $\zeta_M>K/\sqrt{e}$ the asymptotic form Eq. (17) is always greater than $e^{-1/2\omega_e\tau^2}$. [$K/\sqrt{e}\approx 3$, see discussion following Eq. (C5).] For $\zeta_M\le K/\sqrt{e}$ we may therefore match (15) and (17) in a simple way by going from one form to the other at the time τ_M when they are equal. Inspection of Eq. (A19) shows, however, that values of ζ_M as

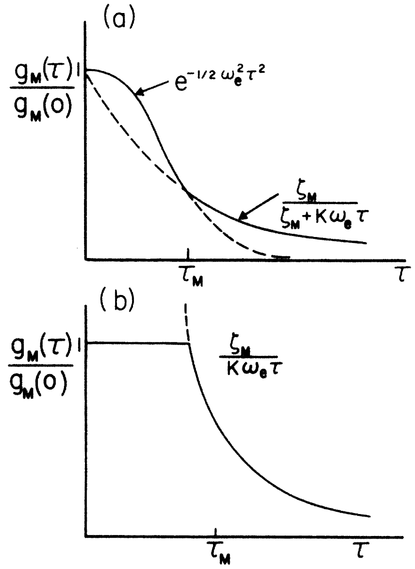

FIG. 3. Matching of short- and long-time portions of $g_M(\tau)$. (a) Solid curve is Eq. (21). Dashed curves represent continuations of functions shown for $\tau > \tau_M$ and $\tau < \tau_M$. (b) Alternate matching procedure. Dashed curve is continuation of $\zeta_M / K\omega_e\tau$ for $\tau < \tau_M$.

large as 17 have to be considered; so a more careful analysis is required.

We consider, therefore, the following simple model which contains the essential physics for large ζ_M. A Gaussian dependence,

$$|F_q^{(M)}|^2 = |F_0^{(M)}|^2 e^{-\alpha^2 q^2}, \tag{19}$$

is assumed, from which we estimate[18] (see Appendix C)

$$g_M(\tau) = \frac{\zeta_M}{\zeta_M + K\omega_e\tau}\, g_M(0) \tag{20}$$

for long times. Equation (20) should represent a considerable improvement over Eq. (17) for the important cases of $\zeta_M > 1$, and it has the virtue that it is now possible to find a finite τ_M at which the forms (15) and (20) are equal. Hence, we take the complete dependence of $g_M(\tau)$ to be

$$\begin{aligned} g_M(\tau) &= g_M(0) e^{-\omega_e^2\tau^2/2}, \qquad \tau \le \tau_M \\ &= g_M(0) \frac{\zeta_M}{\zeta_M + K\omega_e\tau}, \qquad \tau > \tau_M \end{aligned} \tag{21}$$

where τ_M is the time ($\tau_M > 0$) beyond which (20) is larger than (15). This is illustrated in Fig. 3(a).

Equation (21) may now be used in Eq. (6) to obtain an expression for the linewidth. We have, from (21),

$$\int_0^t d\tau (t-\tau) g_0(\tau) = \frac{g_0(0)t}{\omega_e}\left\{\left(\frac{1}{2}\pi\right)^{1/2} \operatorname{erf}\left(\frac{x_0}{\sqrt{2}}\right) + \frac{\zeta_0}{K}\left[\ln\left(\frac{\omega_e t}{x_0 + \zeta_0/K}\right) - 1\right]\right\} \tag{22}$$

and, for $M \ne 0$,

$$\int_0^t d\tau (t-\tau) g_M(\tau) \cos M\omega_0\tau \approx t\int_0^\infty d\tau\, g_M(\tau) \cos M\omega_0\tau$$

$$= \frac{g_M(0)t}{\omega_e}\left\{\left(\frac{1}{2}\pi\right)^{1/2} \operatorname{erf}\left(\frac{x_M}{\sqrt{2}}\right) + \frac{\zeta_M}{K} \times \left[\ln\left(\frac{\omega_e/M\omega_0}{x_M + \zeta_M/K}\right) - 0.577\right]\right\}, \tag{23}$$

where $x_M = \omega_e\tau_M$. The above equations are valid for $\omega_e t \gg x_M$, $\omega_0 t \gg 1$, and $\omega_e/\omega_0 \gg x_M$. These conditions are well satisfied in the region of interest for K_2MnF_4. For $\zeta_M \ll 1$, the conditions $\omega_e t \ll x_M$ and $\omega_e/\omega_0 \gg x_M$ break down, but then the logarithmic terms, in which these approximations are used, become negligibly small anyway. In arriving at Eq. (23) the relation

$$\int_1^\infty (du/u) \cos yu \approx \ln(1/y) - 0.577$$

for $y \ll 1$ has been used.

The final evaluation is performed by using Eqs. (22) and (23), together with values to be found in Appendixes A and C. For numerical constants we have taken $\gamma = 1.76 \times 10^7\ \mathrm{G^{-1}\,sec^{-1}}$, appropriate to the free-electron gyromagnetic ratio which is observed for Mn^{++}, $a = 4.20$ Å, $J/k_B = 4.15$ K (from Breed[9]), $\omega_0/2\pi = 9.3$ and 23.4 GHz, and $S = \frac{5}{2}$. The half-width at half-maximum in magnetic field units ΔH is calculated as $\Delta\omega = \gamma\Delta H = t_0^{-1}$, where t_0 is the time at which the function in square brackets of Eq. (6) has decayed to $1/e$ of its initial value. That is, we assume a Lorentzian line shape. At most a 13% error can be introduced since $\gamma\Delta H = 1.13 t_0^{-1}$ is the calculated value from the line shape at $\theta = 0$ and room temperature (see Fig. 7). Results of the calculation are discussed in Sec. IV along with the experimental data.

In order to test how sensitive the calculation might be to the manner in which the long- and short-time parts of $g_M(\tau)$ are joined together, we have considered an alternate matching procedure, sketched in Fig. 3(b). Here we use Eq. (17) and, for $\zeta_M > K/\sqrt{e}$, simply choose the time τ_M to be such that $\zeta_M / K\omega_e\tau_M = 1$ and assume $g_M(\tau)/g_M(0) = 1$ for $\tau < \tau_M$. For $\zeta_M < K/\sqrt{e}$, τ_M is defined as the larger of the two times for which $e^{-\omega_e^2\tau^2/2} = \zeta_M / K\omega_e\tau$ [see discussion following Eq. (17)]. Results obtained from this approach differ from those using Eq. (21) by less than 10% at any angle; so we conclude that the precise manner in which short- and long-time portions are joined is not overly important.

C. Extension to finite temperature

We assume that above the ordering temperature T_N the basic picture of diffusion for the long wavelength modes at $t \to \infty$ and a short-time Gaussian decay still holds. Also, isotropy of the correlations is maintained in the model. With these assumptions, the formalism used in Sec. II B remains valid except that the quantities D, ω_e, ζ_M, and $g_M(0)$ now must all be regarded as temperature dependent. Their temperature dependence is estimated as follows.

Since[19–21] D is proportional to $q^{-2}\langle\omega_q^2\rangle^{3/2}/\langle\omega_q^4\rangle^{1/2}$ in the limit $q\to 0$, (see also Appendix C) we have

$$\frac{D(T)}{D(\infty)}=\lim_{q\to 0}\frac{\langle\omega_q^2\rangle_T^{3/2}}{\langle\omega_q^2\rangle_\infty^{3/2}}\,\frac{\langle\omega_q^4\rangle_\infty^{1/2}}{\langle\omega^4\rangle_T^{1/2}} \tag{24}$$

for the ratio of D at a temperature T to its value at $T=\infty$. The moments $\langle\omega_q^2\rangle$ and $\langle\omega_q^4\rangle$ are inversely proportional to the static correlation $\langle S_q^z S_{-q}^z\rangle$, and thus we may write in the $q\to 0$ limit

$$\lim_{q\to 0}\frac{\langle\omega_q^n\rangle_T}{\langle\omega_q^n\rangle_\infty}=\frac{1}{f_0}\sum_{r=0}^{\infty}b_r^{(n)}\left(\frac{J}{k_BT}\right)^r, \tag{25}$$

where f_0 is the $q=0$ correlation $\langle S_0^z S_0^z\rangle$ or, equivalently, $\chi_0 T$ normalized to unity at $T=\infty$ and where a high-temperature expansion has been assumed for the numerators of the moments expression, in which $b_0^{(n)}=1$. Collins[22] has derived general formulas for $b_r^{(2)}$ up to and including $r=3$, so that the second moment $\langle\omega_q^2\rangle$ is known to $O(T^{-3})$. He has also obtained the term $b_1^{(4)}$, i.e., the coefficient of T^{-1} for $\langle\omega_q^4\rangle$. We have therefore constructed $D(T)/D(\infty)$ by truncating the series in (25) with the known coefficients. The normalized $\chi_0 T$ is computed from the series coefficients for a classical two-dimensional Heisenberg magnet as given by Stanley.[23] It agrees well with the susceptibility of K_2MnF_4 measured by Breed.[9,24] The resulting temperature dependence of D, together with that of f_0^{-1}, is shown in Fig. 4(a).

Temperature dependence of ζ_M and $g_M(0)$ may be related to that of the static wave-vector correlation,

$$\phi_p(0)=[3/S(S+1)]\langle S_q^z S_{-q}^z\rangle\equiv f_q \tag{26}$$

as in Eqs. (A14) and (A18), within the decoupling approximation. Lee and Liu[25] have performed a Green's-function calculation for a two-sublattice antiferromagnet above T_N. Their result may be expressed in the form

$$f_q=\frac{f_0+\frac{1}{2}(f_s-f_0)(1-\gamma_q)}{1+\lambda(1-\gamma_q^2)}\ , \tag{27}$$

where

$$\gamma_q=Z^{-1}\sum_j e^{i\vec{q}\cdot\vec{r}_{ij}}=\tfrac{1}{2}(\cos q_x a+\cos q_y a)$$

for a system with Z neighbors j coupled to i by the exchange interaction, the latter equality holding for the two-dimensional system of interest. The quantity f_s is the normalized value of $\chi_s T$, where χ_s is the staggered susceptibility, and it is evident that (27) reduces to the correct values at zone center ($\gamma_q=1$) and zone boundary ($\gamma_q=-1$). In Ref. 25 the parameter λ is given by

$$\lambda=\tfrac{1}{4}(f_s-f_0)^2/f_s f_0;$$

however, we find it convenient to choose λ in terms of f_s and f_0 so as to satisfy the sum rule

$$N^{-1}\sum_q f_q=1 \tag{28}$$

for $T>T_N$.

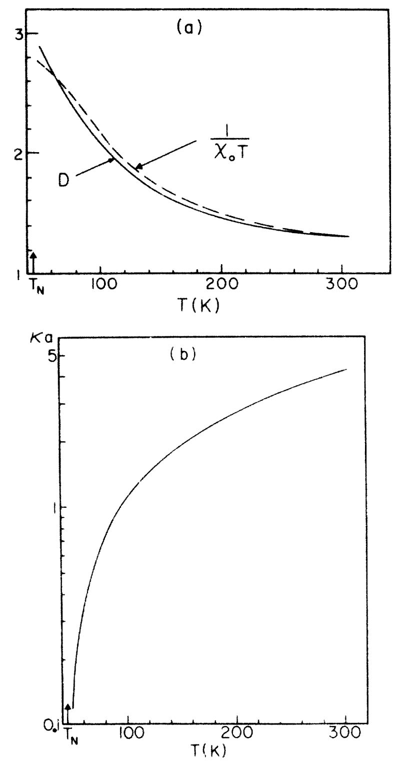

FIG. 4. Theoretical temperature dependence of parameters needed for linewidth calculation. (a) Diffusion coefficient D and $(\chi_0 T)^{-1}$ where χ_0 is uniform susceptibility, both normalized to unity at $T=\infty$. (b) Inverse correlation length κ in units of a.

The assumed f_q in (27) reduces to the familiar Ornstein-Zernicke

$$f_q\propto\frac{1}{q^{*2}+\kappa^2} \tag{29}$$

for $\vec{q}^*=\vec{q}_0-\vec{q}$ near zero [$\vec{q}_0$ is the reciprocal-lattice vector $(\pi/a,\ \pi/a)$]. The inverse correlation length κ is related to λ by $\kappa a=(2/\lambda)^{1/2}$ and is shown in Fig. 4(b) for the values of λ which satisfy (27) and (28). It is known that (29) cannot be correct for a two-dimensional system in the immediate vicinity of T_N, and experiments[26] on K_2NiF_4 have verified this by showing the exponent[27] η to be about 0.4 at T_N. The same data, though, show $\eta=0$ for $T/T_N-1\gtrsim 0.08$, so that Eq. (27), which is consistent with $\eta=0$, should be reasonable except quite near T_N.

The quantity f_s may be obtained from the high-temperature-series expansion[23] of the classical Heisenberg ferromagnet since $f_{s(\text{antiferromagnet})}$

$=f_{0(\text{ferromagnet})}$ for classical spins. Near T_N we have extrapolated the series in the manner done by Lines[28] for our calculation of f_s.

The computations of $g_M(0)$ and ω_e are lengthy at finite temperature because of the presence of the f_q^2 factors. Thus we have restricted the calculation to $\theta=0°$, $55°$ [$\cos^{-1}(1/\sqrt{3})$], and $90°$ and adopted the following numerical procedure. At each temperature λ is computed from (27) and the sum rule (28). This part of the computation is quite rapid and highly accurate since the summation (28) can be converted to a one-dimensional integral involving the zeroth-order Bessel function of imaginary argument.[29] The quantities $g_M(0)$ and ω_e are computed by summing over 6400 points in the two-dimensional Brillouin zone. At each such $\vec{q}$ value the dipole sum $F_q^{(M)}$ is calculated by summing over 400 lattice points.

Detailed results are presented in Sec. IV along with the experimental data. The main features are that the linewidth passes through a minimum as T is decreased, the anisotropy $\Delta H(\theta=0)/\Delta H(\theta=90°)$ also goes through a minimum, and there is no longer a minimum in ΔH vs. θ near $\theta_c=\cos^{-1}(1/\sqrt{3})$ for T close to T_N. These may be explained qualitatively as follows. Since $\Delta\omega$ is dominated at high temperatures by the $q\to 0$ modes, it follows that for an antiferromagnet $\Delta\omega$ should initially decrease as T is lowered. This behavior is to be contrasted with that of a three-dimensional system. In both cases, there is an over-all prefactor of $f_0=\chi_0 T$ in the denominator [see Eqs. (A1)–(A3)]; in three dimensions the sum over all wave vectors $\sum_q |F_q^{(M)}|^2[\phi_q^{(0)}]^2$ tends to be weakly dependent on T. Thus $\Delta\omega$ increases approximately as $(\chi_0 T)^{-1}$ with lowering temperature. However, if most of the contribution comes from $q\approx 0$, as is the case in two dimensions, then $\sum_q |F_q^{(M)}|^2 \times[\phi_q(0)]^2\sim(\chi_0 T)^2$ and an approximate $\chi_0 T$ dependence is expected for $\Delta\omega$. Since the relative strength of $q\approx 0$ modes is decreased with lowering temperature, it follows that the anisotropy will also decrease because, as has been discussed, the $3\cos^2\theta-1$ dependence is characteristic only of $q=0$.

That $\Delta\omega$ passes through a minimum and then increases rapidly as $T\to T_N$ from above is due to the large fluctuations at the wave vector q_0 characteristic of the staggered susceptibility. In this region $f_0\ll f_s$ and the $q\approx 0$ contribution is no longer of much importance. Rather, q_0 dominates and, as a consequence, the situation is qualitatively very similar to that for a three-dimensional antiferromagnet. Also, since the $q\approx 0$ modes are out of the picture, the correlation functions $g_M(\tau)$ no longer have a τ^{-1} tail, and thus both nonsecular ($M\neq 0$) and secular ($M=0$) terms are expected to be important. In this case Huber[30] has shown that the angular dependence of the linewidth reduces to

$$\Delta\omega\propto 1+\cos^2\theta \qquad (30)$$

so that a minimum is no longer expected near $\cos^{-1}(1/\sqrt{3})$ for T close to T_N.

The calculation is not expected to be valid very near T_N since then anisotropy of the fluctuations[26] must be accounted for. Also, it is questionable whether the short-time parameter ω_e can give a reliable estimate of the zero frequency component of $g_M(\tau)$ in the region where decay is strongly influenced by the fluctuations at q_0. In fact, we note that since ω_e as defined in (C1) turns out to be angular dependent near T_N, the anisotropy expressed by (30), which neglects any θ variation of ω_e, is not borne out in our calculations. Rather, we find near T_N $\Delta\omega(\theta=0)/\Delta\omega(\theta=90°)\approx 2.5$ instead of 2.0 as predicted by (30). A treatment of $\Delta\omega$ in terms of critical exponents for $T\to T_N$ has been done elsewhere.[31] The work presented here is likely to be meaningful for $T/T_N-1\gtrsim 0.1$, which corresponds to $T\gtrsim 50$ K for K_2MnF_4.

Qualitative temperature dependence of the linewidth in a two-dimensional ferromagnet is readily discussed in terms of the preceeding formalism. For a ferromagnet the $q\approx 0$ modes grow in strength as temperature is lowered toward the critical point T_c. Hence, opposite to the case of an antiferromagnet, the two-dimensional anomalies become enhanced as T decreases so that $\Delta\omega$ should show a continuous increase with lowering temperature, and the angular anisotropy also should become more pronounced. Once again, this behavior is unlike that of a three-dimensional ferromagnet where the main temperature dependence comes from the $\chi_0 T$ denominator, since the long wavelength modes are not overly important, and hence $\Delta\omega$ decreases with decreasing temperature.

D. Effects of anisotropy and hyperfine couplings

For completeness, comments are in order regarding the contributions of anisotropy and hyperfine interactions to the linewidth. We show below that these are probably negligible.

Single-ion anisotropy is expressed by the Hamiltonian

$$\mathcal{H}_A=\tilde{D}\sum_i S_i^{z'2}, \qquad (31)$$

where z' is the crystalline c axis perpendicular to the plane. The size of $\tilde{D}$ may be estimated from single-ion resonance measurements[32] of Mn^{++} in isomorphous K_2ZnF_4, which yield $\tilde{D}=+35.4\times10^{-4}$ cm^{-1}. Similar measurements[33] on Mn^{++} in another isomorph, K_2MgF_4, give $\tilde{D}=+108\times10^{-4}$ cm^{-1}; however, comparison of lattice parameters indicates that the former figure for $\tilde{D}$ found in K_2ZnF_4 should be more representative of $\tilde{D}$ in concentrated

K_2MnF_4. The pertinent number for the $q=0$ part of the dipole interaction is $\gamma^2\hbar^2\sum_j r_{ij}^{-3} = 2.1\times10^{-1}$ cm^{-1}.

Thus the anisotropy term is only about 2% of the dipolar one and should be negligible. In any event, one may show that single-ion anisotropy produces the same angular dependence of $\Delta\omega$ as the $q=0$ part of the dipolar interaction.

An isotropic hyperfine interaction

$$\mathcal{H}_{hf} = \sum_i A\vec{I}_i \cdot \vec{S}_i , \qquad (32)$$

between electron spin $\vec{S}_i$ and nuclear spin $\vec{I}_i$ gives rise to an isotropic linewidth which may be calculated[17] in terms of the two-spin correlation function $\langle S_i^z(t) S_i^z \rangle$. The calculation proceeds in a manner similar to that described for the dipolar interaction. Two simplifications here are that only two-spin correlation functions are involved and that, since $\mathcal{H}_{hf}$ is a single-ion interaction, the corresponding ζ_M, defined in a manner analogous to Eq. (A18), is unity. From the measured ^{55}Mn NMR frequency in K_2MnF_4, we have[34] $A/\hbar = 1.73\times10^9$ sec^{-1}. This leads to $\Delta H(\text{hf}) = 0.7$ Oe in our computation at infinite temperature and thus the hyperfine contribution is only about 1% of the dipolar linewidth.

III. EXPERIMENT

Experiments were performed on cleaved sections of single crystals of K_2MnF_4 prepared by Ikeda. The 9.3-GHz spectrometer consists of a room-temperature microwave cavity with a cold-finger Dewar in which the sample is placed. The sample could be rotated about the axis of the cold finger with an accuracy of $\pm1^\circ$ of arc. The sample temperature is regulated by the combination of adjusting the flow rate of liquid helium into the cold finger and heating the sample block electrically. The block temperature is controlled by a feedback system using a GaAs diode as the sensing element, and could be held constant within ±0.2 K for several hours. The actual sample temperature was measured by means of a Chromel-Alumel thermocouple, mounted directly on the sample, with the block temperature held constant. Because of the microwave losses in the thermocouple, a separate calibration run was made to determine the sample temperature.

Data at 23.4 and 9.8 GHz were taken with standard K- and X-band spectrometers, respectively, operating at room temperature. These systems, at Sandia, were used to study the frequency dependence of linewidths as presented in Fig. 6. All other measurements referred to were obtained with the above-described 9.3 GHz apparatus at Illinois.

The magnetic field was measured with an NMR gaussmeter at the start and end of each sweep through the resonance line and the resulting curves were fit by a least-squares program to Lorentzian curves. A systematic increase in the rms deviation between the fitted curve and the data was noted as the angle between the sample c axis and the magnetic field departed from 55°. No attempt was made to account for the non-Lorentzian nature of the line in the fitting process so that our linewidths may be systematically in error by an amount which can be of the order of 10% at 0° [see discussion in paragraph following Eq. (23)].

IV. RESULTS

A. Room temperature data

Data are presented in Fig. 5 for the angular variation of the Lorentzian half-width at half-maximum ΔH taken at 9.3 GHz and at 300 K. The solid curve represents a smooth curve drawn through the theoretical values of ΔH at $\theta = 0°$, 55°, and 90° computed for $T = 300$ K. As there are no adjustable parameters in the theory, the comparison is on an absolute basis. The observed linewidth is within 20% of the computed value at all angles and the amplitude of the anisotropy is quite comparable: 30 Oe experimentally as compared with the predicted 40 Oe. The anisotropy amplitude is temperature dependent as may be seen from the $T=\infty$ limit of the linewidth expression which is drawn as a dashed curve on Fig. 5.

The data of Fig. 5 were taken in the a-c plane (azimuthal angle $\varphi = 0$) but, within experimental error, there is no angular variation of the linewidth for fields lying in the basal plane ($\theta = \frac{1}{2}\pi$).

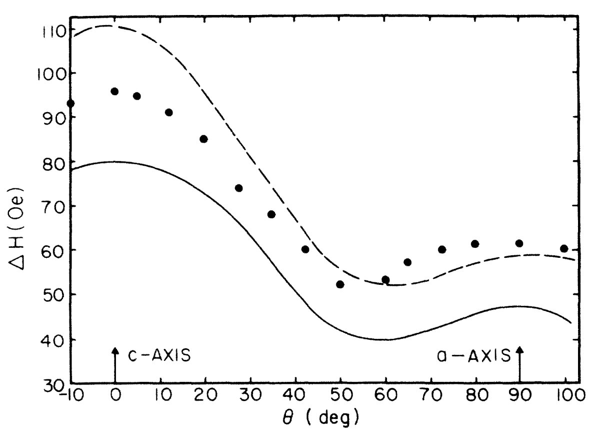

FIG. 5. Angular dependence of linewidth ΔH at room temperature, 9.3 GHz, for field in a-c plane. Dashed curve is theory for infinite temperature. Solid curve is smooth fit through calculated points at $\theta = 0$, 55°, and 90° for 300 K. In this and all successive figures, the theoretical curves contain no adjustable parameters.

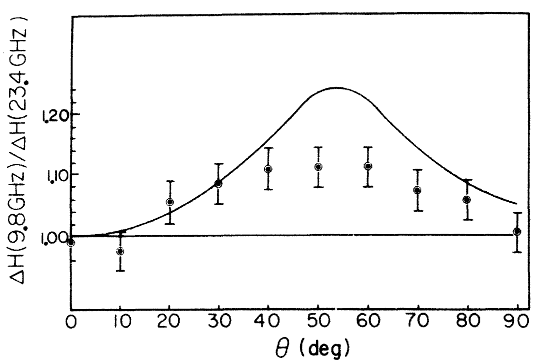

FIG. 6. Frequency dependence of ΔH vs angle θ at room temperature. Solid curve above base line is infinite-temperature theory.

This is consistent with the infinite-temperature calculation which shows that $\Delta H(\varphi = 0)$ differs from $\Delta H(\varphi = \frac{1}{4}\pi)$ by no more than 10%, being 8% at $\theta = \frac{1}{2}\pi$. As previously, the azimuthal angle is measured with respect to the a axis.

A comparison of the linewidth in the a-c plane at 9.8 GHz with that at 23.4 GHz shows a small but systematic narrowing at higher frequency near the minimum angle $\theta = 55°$. In Fig. 6, we show the ratio $\Delta H(9.8\ \mathrm{GHz})/\Delta H(23.4\ \mathrm{GHz})$ measured on the same sample and the theoretical ratio for finite temperature. Despite the relatively large uncertainty in the ratio, there is clear evidence for the predicted effect. The weak maximum in this quantity and the frequency independence of the linewidth at $\theta = 0°$ predicted by Eq. (23) appear to be borne out.

In order to study the room-temperature line shape in detail, direct detection of the cavity level was made (video detection mode). The resultant line shape is known in Fig. 7 by plotting the ratio $I(0)/I(H - H_0)$ vs. $(H - H_0)^2/\Delta H^2$, where H_0 is the field for resonance and $I(0)$ is the amplitude of the absorbtion at H_0. For a Lorentzian line, the data would fall on a straight line of unit slope with an intercept at 1, as shown in Fig. 7. For reference, a Gaussian, which falls off much faster in the wings, is also shown. The data at $\theta = 55°$ follow the Lorentzian shape to within experimental uncertainty as was indicated by the smaller rms deviations of data taken at $\theta = 55°$ from Lorentzian curves. Theory predicts a Lorentzian shape at $\theta = \cos^{-1}(1/\sqrt{3}) = 55°$ since at that angle the amplitude of the $q = 0$ secular component of the perturbation is zero, which makes $\zeta_0 = 0$.

For fields along the c axis ($\theta = 0$) the line shape was given by (6) and can be written

$$I(H - H_0) \sim \mathfrak{F}\{\exp(-At - Bt\ln t/t_0)\},$$

where the parameters A, B, and t_0 can be identified from a comparison with (22) and (23), and $(H - H_0)$ is associated with $(\omega - \omega_0)/\gamma$. Using values of A, B, and t_0 appropriate to 300 K and 9.3 GHz we obtain the theoretical line shape given by the dashed line of Fig. 7. Good agreement is seen to exist both at $\theta = 0°$ and at $\theta = 55°$. It is interesting to note that since the relative size of A and B is important, no single curve for the line shape holds for all linewidths of an ideal two-dimensional system at $\theta = 0$ as is the case for the linear chain (i.e., the Fourier transform of $e^{-t^{3/2}}$). This fact was not appreciated in our earlier publication[35] and consequently we displayed a theoretical line shape for arbitrary A/B which did not give satisfactory agreement with experiment.

B. Temperature dependence

The temperature dependence of the linewidth was measured at 9.3 GHz for $\theta = 0°$, 55°, and 90° over the temperature range 50–170 K. The results are shown in Figs. 8 and 9 which give, respectively, the linewidth at $\theta = 0°$ and the anisotropy expressed by the ratios $\Delta H(\theta = 0)/\Delta H(\theta = 90°)$ and $\Delta H(\theta = 90°)/\Delta H(\theta = 55°)$. As predicted in Sec. II C, the linewidth has a broad minimum near 100 K before rising sharply as the Néel temperature is approached. The theoretical linewidths for these angles were calculated at several temperatures using the procedure discussed in Sec. II C. The results are shown as the curves in Figs. 8 and 9, again without adjustable parameters. The agree-

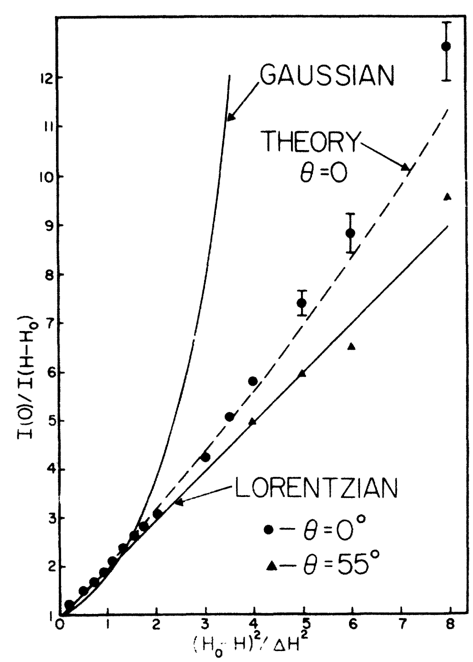

FIG. 7. Line shape at room temperature, 9.3 GHz.

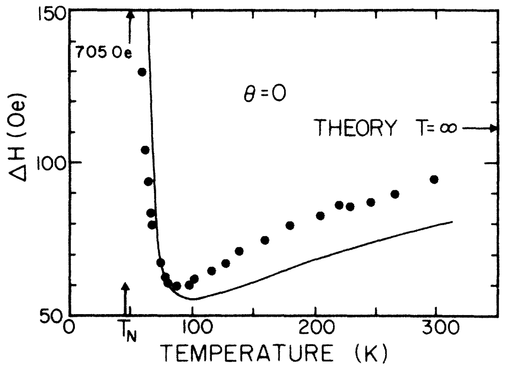

FIG. 8. Temperature dependence of linewidth for $\theta=0$. Solid curve is theory. ΔH reaches 705 Oe as indicated at 50 K$\approx 1.1T_N$.

ment at room temperature extends to 60 K with agreement to within 10 Oe at all angles. We take this as ample confirmation of the applicability of the diffusion-dominated exchange narrowing model presented above to nearly two-dimensional antiferromagnets such as K_2MnF_4.

At lower temperatures, the theoretical analysis presented above indicated that the dominance of $q=0$ modes, which leads to the minimum in the linewidth at $\theta=55°$, will give way to fluctuations at the antiferromagnetic wave vector q_0. The crossover is clearly seen in the data to occur near 70 K at which temperature the linewidth is the same for $\theta=55°$ and $\theta=90°$. This is quite close to the predicted value of 75 K. The predicted temperature dependence of $\Delta H(\theta=0)/\Delta H(\theta=90°)$ is also in reasonable agreement with experiment. We note that at the lowest temperature the value $\Delta H(\theta=0)/\Delta H(\theta=90°)=2.5$ exceeds the figure of 2.0 predicted by Eq. (30), which assumes complete dominance of modes at the antiferromagnetic wave vector. A ratio greater than 2.0 has been observed[15] in $NiCl_2$ near T_N, and is accounted for in Huber's theory[30] by the damping rate of the mode q_0 becoming comparable to ω_0 in the critical region. In our calculation, an additional mechanism is the angular dependence of ω_e. Although it is interesting that there is exact agreement of our theory with experiment for $\Delta H(\theta=0)/\Delta H(\theta=90°)$ at the lowest temperature, this may be fortuitous since, as mentioned, we do not expect our method to hold in the immediate vicinity of T_N.

The temperature dependence observed here is in agreement with that found by Yokozawa[36] and by deWijn *et al.*[37] for K_2MnF_4, and is similar to that reported in Ref. 10 for other two-dimensional antiferromagnets. The low-temperature angular dependence, which does not show a minimum at $\theta=55°$, was also reported in Ref. 37.

C. Frequency shift

Figure 10 shows the field H_0 required for resonance vs. θ. There are two mechanisms for this angular variation which we refer to as classical and dynamical. The classical effect simply comes from the mean dipolar field,

$$H_{\rm dip}=\langle\mu_z\rangle\sum_j(3\cos^2\theta_{ij}-1)r_{ij}^{-3}\ , \tag{33}$$

where the average moment $\langle\mu_z\rangle$ is given by

$$\langle\mu_z\rangle=\frac{\gamma^2\hbar^2S(S+1)H_0}{3k_B(T+\Theta_W)} \tag{34}$$

in the high-temperature regime with Θ_W the Curie-Weiss temperature ≈ 96 K for K_2MnF_4. The field $H_{\rm dip}$ adds to the applied field and thus produces a shift $\delta H_0=-H_{\rm dip}$ in the field required for resonance at a fixed frequency. For a two-dimensional lattice appropriate to K_2MnF_4 we find at 300 K and for a free electron $g=2.00$,

$$\delta H_0\approx 0.4\,\nu(3\cos^2\theta-1)\ , \tag{35}$$

where ν is the frequency in GHz and δH_0 is measured in Oe.

This relation is plotted as the dashed lines in Fig. 10 for the two frequencies, and it is seen that the angular variation of H_0 is satisfactorily accounted for in this manner. The g factors at 60° are 2.007 and 1.998 at X- and K-band frequencies, respectively.

The agreement may be somewhat fortuitous since

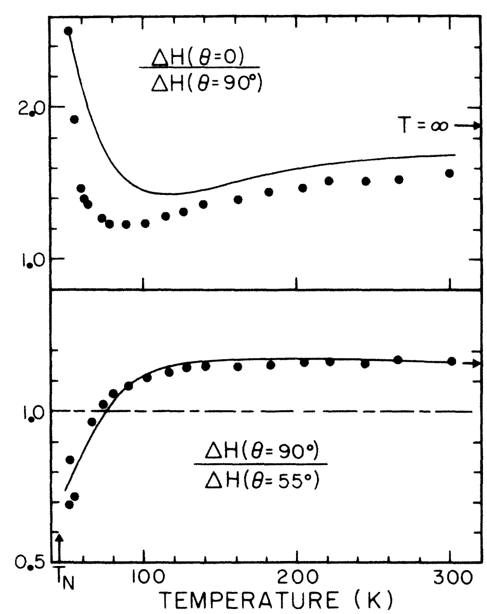

FIG. 9. Temperature dependence of linewidth anisotropy. Solid curves are theoretical, with infinite temperature points shown by arrows.

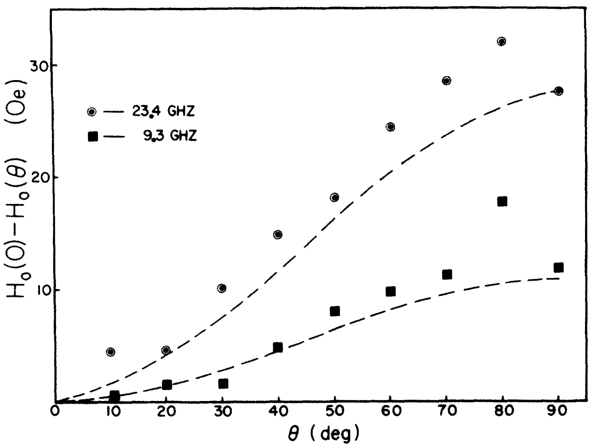

FIG. 10. Angular dependence of field H_0 required for resonance, referred to its value at $\theta=0$, at room temperature. Dashed curves represent the shifts expected at the two frequencies from the classical dipolar field, Eq. (35).

we have not included surface demagnetizing fields which can contribute an amount of the order of $4\pi M_s$ to H_{dip} where the magnetization per volume is $M_s = 2\langle\mu_z\rangle/a^2c$ for the K_2MnF_4 structure with lattice constants a and c (two spins per unit cell). At room temperature $4\pi M \approx 6$ Oe at 9.3 GHz, so the effect of sample shape on the angular variation of H_0 can be important.

The second, dynamical, effect comes from the exchange narrowing phenomenon itself. Equation (6) gives only the relaxation part of $\chi''(\omega)$. A more complete expression[4,38] shows that there is a frequency shift ,

$$\delta\omega = -\sum_{m=-2}^{2}\int_0^\infty d\tau \, \sin M\omega_0\tau \, \hat{g}_M(\tau) \, , \tag{36}$$

where g_M of Eq. (6) is related to $\hat{g}_M$ by $g_M = \hat{g}_M + \hat{g}_{-M}$.

The upper limit in (36) has been extended to ∞ for the reason discussed after Eq. (7). The field shift $\delta H = -\delta\omega/\gamma$ may then be computed by using Eq. (21) in Eq. (36). The resulting dynamical effect predicted for infinite temperature is shown in Fig. 11. This contribution to the shift is approximately independent of frequency since it is nearly proportional to the frequency-independent integral $\int_0^\infty \sin\omega_0\tau (d\tau/\tau)$. It is most likely that its magnitude of 7 Oe maximum is too small to be observed in comparison with the shift from H_{dip} at these frequencies. Thus we cannot make meaningful comparison here between theory and experiment for the more interesting dynamical shift. Such a study could be made by going to much lower frequencies where H_{dip} is diminished or by making careful measurements of g-factor vs. angle at several frequencies as done by Henderson and Rogers.[38]

V. SUMMARY AND CONCLUSIONS

We have measured the ESR linewidth ΔH in a single crystal of K_2MnF_4 as a function of the angle θ between $\vec{H}$ and the c axis, as well as of the azimuthal angle φ and as a function of temperature. The angular dependence is independent of φ and at high temperatures is proportional to $(3\cos^2\theta - 1)^2$ plus a constant term. As the temperature T is lowered, the linewidth initially decreases, passes through a minimum, and increases rapidly as T approaches T_N. The angular dependence of ΔH is also temperature dependent such that $\Delta H(\theta = 55°)$ becomes greater than $\Delta H(\theta = 90°)$ at the lower temperatures. The line shape has also been studied at high temperatures, and we find a Lorentzian line at $\theta = 55°$ but a significant departure from Lorentzian at $\theta = 0$. Measurements at 23.4 and 9.8 GHz reveal that $\Delta H(\theta = 0)$ is independent of frequency but $\Delta H(\theta = 55°)$ is noticeably more narrow at the higher frequency.

The above results have been interpreted in terms of a two-dimensional Heisenberg antiferromagnet, and good agreement has been obtained for all aspects of the data. In particular we note that the absolute value of ΔH has been calculated to within 20% at all angles and over a broad range of temperature using only the classical dipolar interaction and measured exchange constant, with no adjustable parameters. The method was to use spin time correlation functions in the general resonance formula which are diffusive for long times and Gaussian for short times. A notable feature is that the observed angular dependence cannot be obtained by considering the zero-time values of the correlation functions. These involve a sum over all wave vectors and predict, for $\varphi = 0$, ΔH to be greater at $\theta = \frac{1}{2}\pi$ than at $\theta = 0$. The long wavelength $q \to 0$ components do, however, show the proper dependence, and these are expected to dominate the long-time behavior. Thus we have rather conclusive evidence from this study of a two-dimensional compound that the long wave-

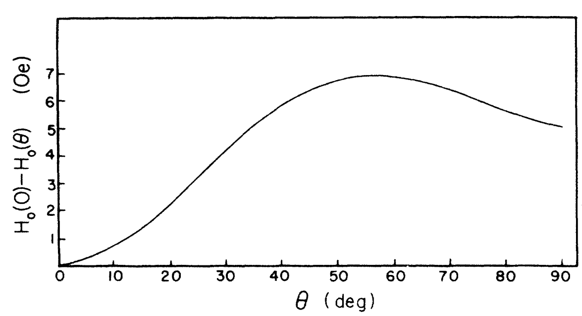

FIG. 11. Theoretical angular dependence of H_0 due to the dynamical shift, Eq. (36), at infinite temperature.

length modes control the relaxation processes in the region where the asymptotic $\tau^{-d/2}$ dependence is important. Evidence of quite this direct a nature is not possible for a one-dimensional system since there all wavelengths produce the same angular dependence.

The dependence of resonance field upon θ has likewise been observed. It can be explained quantitatively by the net dipolar field present in noncubic K_2MnF_4. The perhaps more interesting frequency shift which arises from the two-dimensional spin dynamics is masked by this mean field at the high frequencies used here and thus has not been measured.

In conclusion, our results show that the recent theories of spin dynamics, which include the diffusive behavior of long wavelength modes, can be applied with quantitative success to the two-dimensional antiferromagnet above the ordering temperature, at least as long as we are not in the immediate vicinity of T_N. It should be mentioned, however, that although there is very good agreement for the antiferromagnet, our formalism does not appear to be satisfactory for the two-dimensional ferromagnets studied thus far. Recent measurements on K_2CuF_4[39] and $NiCl_2$,[15] which have ferromagnetic interactions within the plane, show a linewidth which initially decreases as T is lowered from a high value, whereas we would predict an initial increase of ΔH for a ferromagnet. It might be that the difficulty is associated with the non-S-state character of the ions in these materials, for which nondipolar broadening can be important. Also, interplane interactions may be more effective in K_2CuF_4 and $NiCl_2$ than in K_2MnF_4 so that the strong two-dimensional effects are washed out.

ACKNOWLEDGMENTS

D. Cooper and R. Herman provided valuable technical assistance and help with the measurements.

APPENDIX A: DIPOLE CONTRIBUTION TO $g_M(\tau)$

The various g_M are given by[4,40]

$$g_0(\tau)=\tfrac{3}{4}\gamma^4\hbar^2 f_0^{-1}S(S+1)N^{-1}\sum_{qq'}F_q^{(0)}F_{q'}^{(0)}\mathcal{S}_{qq'}^{(0)}(\tau), \quad (A1)$$

$$g_1(\tau)=\tfrac{15}{2}\gamma^4\hbar^2 f_0^{-1}S(S+1)N^{-1}\sum_{qq'}F_q^{(1)}F_{q'}^{(-1)}\mathcal{S}_{qq'}^{(1)}(\tau), \quad (A2)$$

$$g_2(\tau)=\tfrac{3}{4}\gamma^4\hbar^2 f_0^{-1}S(S+1)N^{-1}\sum_{qq'}F_q^{(2)}F_{q'}^{(-2)}\mathcal{S}_{qq'}^{(2)}(\tau), \quad (A3)$$

where

$$F_q^{(0)}=\sum_j(3\cos^2\theta_{ij}-1)r_{ij}^{-3}e^{i\vec{q}\cdot\vec{r}_{ij}}, \quad (A4)$$

$$F_q^{(1)}=\sum_j\sin\theta_{ij}\cos\theta_{ij}e^{-i\varphi_{ij}}r_{ij}^{-3}e^{i\vec{q}\cdot\vec{r}_{ij}}, \quad (A5)$$

$$F_q^{(2)}=\sum_j\sin^2\theta_{ij}e^{-2i\varphi_{ij}}r_{ij}^{-3}e^{i\vec{q}\cdot\vec{r}_{ij}}, \quad (A6)$$

in which θ_{ij} and φ_{ij} are polar and azimuthal angles, respectively, of $\vec{r}_{ij}$ with respect to a coordinate system in which the applied field $\vec{H}$ is along the polar axis.

The spin correlation functions are

$$\mathcal{S}_{qq'}^{(0)}(\tau)=\mathcal{S}_{qq'}^{(2)}(\tau)=\tfrac{1}{2}\langle S_q^z(\tau)S_{-q}^+(\tau)S_{q'}^z S_{-q'}^-\rangle/[\tfrac{1}{3}S(S+1)]^2, \quad (A7)$$

$$\mathcal{S}_{qq'}^{(1)}(\tau)=\tfrac{1}{20}\{\langle[S_q^+(\tau)S_q^-(\tau)-2S_q^z(\tau)S_{-q}^z(\tau)]\times(S_{q'}^-S_{q'}^+-2S_{q'}^zS_{-q'}^z)\rangle+\langle S_q^+(\tau)S_{-q}^+(\tau)S_{q'}^-S_{-q'}^-\rangle\}/[\tfrac{1}{3}S(S+1)]^2. \quad (A8)$$

Upon RPA decoupling of the four-spin correlations the sums all reduce to

$$\sum_{qq'}F_q^{(M)}F_{q'}^{(-M)}\mathcal{S}_{qq'}^{(M)}(\tau)=\sum_q|F_q^{(M)}|^2\langle S_q^z(\tau)S_{-q}^z\rangle^2/[\tfrac{1}{3}S(S+1)]^2 \quad (A9)$$

for isotropic correlations ($\langle S_q^z(\tau)S_{-q}^z\rangle=\tfrac{1}{2}\langle S_q^+(\tau)S_q^+\rangle$). In Eqs. (A7) and (A8) time dependence is with respect to the Heisenberg-exchange Hamiltonian only. Zeeman modulation has been explicitly accounted for in Eq. (6).

Note that all g_M are divided by

$$f_0=3\langle S_0^zS_0^z\rangle/S(S+1)=\chi_0T/[\tfrac{1}{3}N\gamma^2\hbar^2S(S+1)k_B^{-1}], \quad (A10)$$

which is the normalized ($f_0=1$ at $T=\infty$) $q=0$ correlation or χ_0T, where χ_0 is the static uniform susceptibility.

Angular dependence of both $g_M(0)$ and the $q\to0$ part $|F_0^{(M)}|^2\langle S_0^zS_0^z\rangle^2$ enter into the expressions for the two-dimensional linewidth. They represent, respectively, the short-time and long-time properties of $g_M(\tau)$. Since

$$g_M(0)\propto f_0^{-1}\sum_q|F_q^{(M)}|^2\langle S_q^zS_{-q}^z\rangle^2, \quad (A11)$$

simple analytic expressions cannot be given at finite temperature where $\langle S_q^zS_{-q}^z\rangle$ is a function of q. But in the infinite-temperature limit, where $\langle S_q^zS_{-q}^z\rangle=\tfrac{1}{3}S(S+1)$ independent of q, we have

$$g_0(0)=\tfrac{3}{16}\gamma^4\hbar^2S(S+1)[(1-3\cos^2\theta)^2+9\sin^4\theta]\sum_j r_{ij}^{-6}, \quad (A12)$$

$$g_1(0)=\tfrac{15}{4}\gamma^4\hbar^2S(S+1)\sin^2\theta\cos^2\theta\sum_j r_{ij}^{-6}, \quad (A13)$$

$$g_2(0)=\tfrac{3}{4}\gamma^4\hbar^2S(S+1)(\cos^2\theta+\tfrac{1}{2}\sin^4\theta)\sum_j r_{ij}^{-6}. \quad (A14)$$

It is convenient to consider the ratios

$$\zeta_M=|F_0^{(M)}|^2\langle S_0^zS_0^z\rangle^2\Big/\Big(N^{-1}\sum_q|F_q^{(M)}|^2\langle S_q^zS_{-q}^z\rangle^2\Big), \quad (A15)$$

which, in the high-temperature limit, are

$$\zeta_0=b\,\frac{(1-3\cos^2\theta)^2}{(1-3\cos^2\theta)^2+9\sin^4\theta}, \quad (A16)$$

$$\zeta_1=\tfrac{1}{2}b, \quad (A17)$$

$$\zeta_2 = \frac{\frac{1}{4}b \sin^4\theta}{\cos^2\theta + \frac{1}{2}\sin^4\theta} , \tag{A18}$$

where

$$b \equiv \left(\sum_j r_{ij}^{-3}\right)^2 \Big/ \sum_j r_{ij}^{-6} \tag{A19}$$

has the value 17.58 for a square lattice. Equations (A12)–(A14) and (A16)–(A18) are for $\vec{H}$ in a (100) plane ($\varphi = 0$) and assume $\langle \cos^4\varphi'_{ij}\rangle_{av} = \frac{1}{2}$ (see Fig. 1).

APPENDIX B: CORRELATION FUNCTIONS FOR $\tau \to \infty$

The correlation function $g_0(\tau)$ is given by

$$g_0(\tau) \propto \sum_{q,q'} F_q^{(0)} F_{q'}^{(0)} \langle S_q^z(\tau) S_{-q}^+(\tau) S_{q'}^z S_{q'}^- \rangle$$
$$= \sum_{q,q'} F_q^{(0)} F_{q'}^{(0)} \langle S_q^z S_{-q}^+ S_{q'}^z(-\tau) S_{q'}^-(-\tau)\rangle. \tag{B1}$$

From (B1) it follows that if $g_0(\tau)$ is dominated by $q \to 0$ in the $\tau \to \infty$ limit, then it is also dominated by $q' \to 0$ in the same limit [at least at high temperatures where $g_0(\tau)$ must be an even function of τ]. That the major contribution to $g_0(\tau)$ is from $q \to 0$ for sufficiently long times is a consequence of $\vec{S}_q(\tau)$ being a constant of the motion at $q = 0$ and of the relative importance of small q in lower dimensions.

We therefore assert that for $\tau \to \infty$ both $F_q^{(0)}$ and $F_{q'}^{(0)}$ can be replaced by their $q, q' = 0$ values in the expression for $g_0(\tau)$ and thus a $(3\cos^2\theta - 1)^2$ contribution to the angular dependence results, irrespective of whether or not decoupling of the four-spin time correlations is valid.

APPENDIX C: SHORT- AND LONG-TIME BEHAVIOR OF $g_M(\tau)$

The effective Gaussian frequency ω_e of Eq. (15) is given by

$$\omega_e^2 = -\ddot{g}_M(0)/g_M(0)$$
$$= 2\sum_q |F_q^{(M)}|^2 \langle \omega_q^2\rangle f_q^2 \Big/ \sum_q |F_q^{(M)}|^2 f_q^2 , \tag{C1}$$

where

$$f_q = 3\langle S_q^z S_{-q}^z\rangle / S(S+1)$$

and the wave-vector second moment is

$$\langle \omega_q^2\rangle = -\langle \ddot{S}_q^z(0) S_{-q}^z\rangle / \langle S_q^z S_{-q}^z\rangle . \tag{C2}$$

It has been assumed that $\langle\omega_q^2\rangle \gg \langle\omega_q\rangle^2$, where $\langle\omega_q\rangle = -i\langle \dot{S}_q^z(0) S_{-q}^z\rangle / \langle S_q^z S_{-q}^z\rangle$, which is valid at high temperatures.

At infinite temperature we have

$$\langle\omega_q^2\rangle = \tfrac{16}{3} S(S+1) J^2 (2 - \cos q_x a - \cos q_y a) \tag{C3}$$

from the calculations of Collins and Marshall[41] particularized to a square lattice with a nearest-neighbor exchange interaction $-2J\vec{S}_i \cdot S_j$ and lattice constant a. Use of (C3) in (C1) gives

$$\omega_e^2 = \tfrac{64}{3} S(S+1) J^2 (1 - \Delta_M) \tag{C4}$$

at infinite temperature where Δ_M is a correction of the order of 0.2 which arises from the $\cos q_x a - \cos q_y a$ part of (C3). The diffusion coefficient D for the long-time dependence of Eq. (16) has been calculated by several authors[19–21] who find that it is proportional to

$$\lim_{q\to 0} q^{-2} \langle\omega_q^2\rangle^{3/2} / \langle\omega_q^4\rangle^{1/2} ,$$

where $\langle\omega_q^4\rangle$ is the fourth moment. Only slight differences are found in the constant of proportionality depending on the particular method. Use of results of Ref. 41 for $\langle\omega_q^4\rangle$ in a square lattice and the Tahir-Kheli and McFadden[21] constant of proportionality then gives

$$D = \tfrac{1}{3}(2\pi)^{1/2} J a^2 [S(S+1)]^{1/2} \tag{C5}$$

for large spin values $\{3/[8S(S+1)] \ll 1\}$ and infinite temperature. Equations (C5) and (C6) show that the constant K defined in (17) has a value of about 5.0.

The long-time behavior is obtained by using Eq. (16) in Eqs. (A1) and (A9) and converting the summations to integrations over the first Brillouin zone of a square lattice. Thus we have at high temperature

$$g_0(\tau) = \tfrac{3}{4}\gamma^4\hbar^2 S(S+1)(a/\pi)^2 \int_0^{\pi/a}\int_0^{\pi/a} dq_x\, dq_y$$
$$\times |F_q^{(0)}|^2 \exp[-2D(q_x^2 + q_y^2)\tau] , \tag{C6}$$

with similar expressions for $g_1(\tau)$ and $g_2(\tau)$. For $\tau \to \infty$ the upper limits may be extended to infinity and, since the major contribution is for $\vec{q}$ near zero, $|F_q^{(0)}|^2$ may be replaced by $|F_0^{(0)}|^2$. The result may be written as

$$\lim_{\tau\to\infty} g_M(\tau) = g_M(0)\zeta_M / (8\pi D\tau/a^2) \tag{C7}$$

for ζ_M as defined in (A18).

If a Gaussian dependence

$$|F_q^{(M)}|^2 = |F_0^{(M)}|^2 e^{-\alpha^2 q^2} \tag{C8}$$

is used, then it is evident that the denominator of (C7) is modified to $(8\pi D\tau + 4\pi\alpha^2)/a^2$. However, according to (A18) we would have

$$\zeta_M = (\pi/a)^2 \Big/ \int_0^{\pi/a}\int_0^{\pi/a} dq_x\, dq_y\, e^{-\alpha^2 q^2} = 4\pi\alpha^2/a^2 \tag{C9}$$

for $\pi^2\alpha^2/a^2 \gtrsim 2$ so that the form (20) results.

---

*Work supported in part by the U. S. Atomic Energy Commission (Sandia) and by NSF Grant No. GH33634.

[1] See, for example, M. T. Hutchings, G. Shirane, R. J. Birgeneau, and S. L. Holt, Phys. Rev. B 5, 1999 (1972) and K. Takeda, S. Matsukawa, and T. Haseda, J. Phys. Soc. Jap. 30, 1330 (1971) for recent studies of some one-dimensional compounds.

[2] A list of several two-dimensional compounds has been compiled by L. J. deJongh, P. Bloembergen, and J. J. H. P. Colpa, Physica 58, 305 (1972).

[3] P. W. Anderson and P. R. Weiss, Rev. Mod. Phys. 25, 269 (1953).

[4] R. Kubo and K. Tomita, J. Phys. Soc. Jap. 9, 888 (1954).

[5] L. P. Kadanoff and P. C. Martin, Ann. Phys. (N. Y.) 24, 419 (1963).

[6] R. E. Dietz, F. R. Merritt, R. Dingle, D. Hone, B. G. Silbernagel, and P. M. Richards, Phys. Rev. Lett. 26, 1186 (1971).

[7] R. R. Bartkowski, M. J. Hennessy, B. Morosin, and P. M. Richards, Solid State Commun. 11, 405 (1972).

[8] J. H. VanVleck, Phys. Rev. 74, 1168 (1948).

[9] D. J. Breed, Physica 37, 35 (1967).

[10] H. P. Boesch, U. Schmocker, F. Waldner, K. Emerson, and J. E. Drumheller, Phys. Lett. A 36, 461 (1971).

[11] Equation (6) represents the first term in a comulant expansion. The higher terms have been shown by Kubo [R. Kubo, in ***Fluctuation, Relaxation and Resonance in Magnetic Systems***, edited by D. ter Haar (Plenum, New York, 1962)] to be negligible if $g_M(\tau)$ decays rapidly compared with the observed relaxation time. The slow long-time decay of $g_M(\tau)$ in low dimensions can, however, raise questions as to the validity of Eq. (6). Reiter (G. F. Reiter, private communication) has considered this problem and derived a self-consistent expression for the line shape which, within certain approximations, includes all the higher-order cumulants. He finds a fairly significant deviation from (6) in one dimension, but the difference is practically negligible for two dimensions. In view of this, it appears that the Kubo-Tomita formula is at least a satisfactory starting point.

[12] D. Hone, AIP Conf. Proc. 5, 413 (1972).

[13] M. J. Hennessy, C. D. McElwee, and P. M. Richards, Phys. Rev. B 7, 930 (1973).

[14] K. Kawasaki, Prog. Theor. Phys. 39, 285 (1968); D. L. Huber, J. Phys. Chem. Solids 32, 2145 (1971).

[15] R. J. Birgeneau, L. W. Rupp, Jr., H. J. Guggenheim, and P. A. Lindgard, Phys. Rev. Lett. 30, 1252 (1973).

[16] It has been claimed in Ref. 15 that the ESR linewidth in $NiCl_2$ near the critical point gives evidence for the failure of four-spin decoupling. However, Kawasaki [K. Kawasaki, Phys. Lett. A 26, 543 (1968)] apparently has a theory, as yet unpublished in detail, which reproduces the $NiCl_2$ data by using decoupling together with a proper summation over the whole Brillouin zone. We are grateful to R. J. Birgeneau for conveying this information about Kawasaki's work.

[17] J. E. Gulley, D. Hone, D. J. Scalapino, and B. G. Silbernagel, Phys. Rev. B 1, 1020 (1970).

[18] Equation (20) here differs from Eq. (4.27) of Ref. 17 (apart from the difference caused by dimensionality) in that we have the form $g_m(t) = C(t+t_0)^{-d/2}$ whereas one finds $g_M(t) = C(t-t_0)^{-d/2}$ in the paper of Gulley *et al.*, t_0 being an appropriate time $t_0 > 0$ and C an appropriate constant in either case. We believe that our version is more satisfactory since it seems reasonable that for $t \gtrsim t_0$ the true $g_M(t)$ should be less than the asymptotic value $Ct^{-d/2}$ because the expression $Ct^{-d/2}$ assumes that all modes decay at the slow diffusive rate rather than the more rapid Gaussian one. Also, of course, our expression can in principle be applied for all $t > 0$ whereas the one of Ref. 17 becomes physically unacceptable near t_0.

[19] P. G. deGennes, J. Phys. Chem. Solids 4, 223 (1958).

[20] H. S. Bennett and P. C. Martin, Phys. Rev. 138, A608 (1965).

[21] R. A. Tahir-Kheli and D. G. McFadden, Phys. Rev. 182, 604 (1969).

[22] M. F. Collins, Phys. Rev. B 4, 1588 (1971).

[23] H. E. Stanley, Phys. Rev. 158, 546 (1967).

[24] D. J. Breed, Phys. Lett. 23, 181 (1966).

[25] K. H. Lee and S. H. Liu, Phys. Rev. 159, 390 (1967).

[26] R. J. Birgeneau, J. Skalyo, Jr., and G. Shirane, Phys. Rev. B 3, 1736 (1971).

[27] M. E. Fisher and R. J. Burford, Phys. Rev. 156, 583 (1967).

[28] M. E. Lines, Phys. Rev. B 3, 1749 (1971).

[29] E. Montroll, *Proceedings of the Third Berkeley Symposium on Mathematical Statistics and Probability* (University of California Press, Berkeley, Calif., 1956), Vol. III.

[30] D. L. Huber, Phys. Rev. B 6, 3180 (1972); Phys Rev. A 43, 311 (1973).

[31] D. L. Huber and M. S. Seehra, Phys. Lett.; P. M. Richards, Solid State Commun. 13, 253 (1973).

[32] V. J. Folen, Phys. Rev. B 6, 1670 (1972).

[33] A. H. M. Schrama, P. I. J. Wouters, and H. W. deWijn, Phys. Rev. B 2, 1235 (1970).

[34] H. W. deWijn, R. E. Walstedt, L. R. Walker, and H. J. Guggenheim, J. Appl. Phys. 42, 1595 (1971).

[35] M. B. Salamon and P. M. Richards, AIP Conf. Proc. 10, 187 (1973).

[36] Y. Yokozawa, J. Phys. Soc. Jap. 31, 1590 (1971).

[37] H. W. deWijn, L. R. Walker, J. L. Davis, and H. J. Guggenheim, Solid State Commun. 11, 803 (1972).

[38] A. J. Henderson, Jr. and R. N. Rogers, Phys. Rev. 152, 218 (1966).

[39] I. Yamada and M. Ikebe, J. Phys. Soc. Jap. 33, 1334 (1972).

[40] See, for example, A. Abragam, *Principles of Nuclear Magnetism* (Oxford U. P., New York, 1961); C. P. Slichter, *Principles of Magnetic Resonance* (Harper and Row, New York, 1963).

[41] M. F. Collins and W. Marshall, Proc. Phys. Soc. (Lond.) 92, 390 (1967).